Journal of Population Therapeutics & Clinical Pharmacology

RESEARCH ARTICLE
DOI: 10.53555/2grmn421

EXPLORATION OF THE GOLD NANOPARTICLES–DNA INTERACTION: A NOVEL APPROACH TOWARDS RAPID CANCER DIAGNOSIS

Tahira Ahmed[1*], Yasir Jamil[1], Sajid Bashir[2], Yasir Javed[1], And Amer Jamil[1]

[1*]University of Agriculture Faisalabad, Pakistan.
[2]Pakistan Insititute of Nuclear Medicine (PINUM)

***Corresponding Author:** Tahira Ahmed
Email: syedatahira25@yahoo.com

Abstract: Unique optical, physical, and biological characteristics of gold nanoparticles make them suitable for use in medicine, particularly in the detection of cancer. This study synthesized spherical monodispersed gold nanoparticles (AuNPs) by extending a little from established Turkevich, Frens via varying the concentration of HAuCl4/Citrate ratios. These freshly synthesized red color AuNPs are further characterized for size, size distribution, shape and monodispersity by UV/Vis spectrophotometer, DLS, TEM and AFM studies. Next genomic DNA was extracted from cancer and normal individuals' blood samples by standard protocol and is further characterized by Nano Drop spectrophotometer. It was hypothesized that DNA has diverse tendencies to get adsorb onto AuNPs surface in colloidal solution form. Using this observation, we had planned this novel project based on color variations related to interaction of 40nm citrate capped AuNPs conjugated to non-functionalized genomic DNA both from cancer and normal samples. SPR peak stability vs SPR shift towards longer wavelength upon salt addition has been studied thoroughly, so this novel spectroscopic technique analyzed sample data set (both cancer and normal genomic DNA) adsorption and it was observed to show parabolic trend with SPR peak stability at 536nm in almost all Breast cancer samples where solution color remained red upon salt addition, so this led the basis of cancer detection, while healthy samples showed broadened SPR peak with diminished absorption values at SPR peak showing particle aggregation visible to eye as blue/grey color. Analysis results obtained from colorimetry and UV/Vis spectroscopy for monodisperse to polydisperse AuNPs colloidal solution expose that bigger AuNPs, that make the major volume of the solution, could overshadow the presence of smaller ones and maybe we need higher concentration of DNA to stabilize these AuNPs against aggregation upon salt addition.

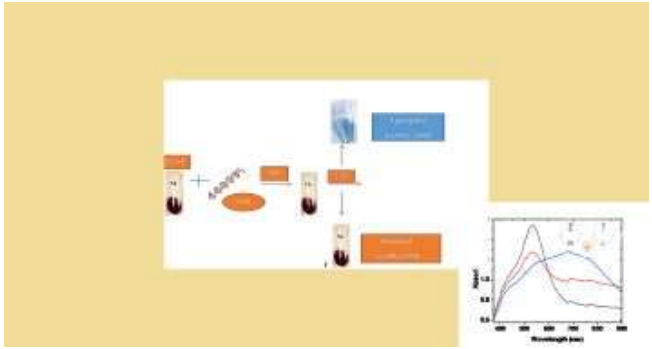

• **Keywords:** DNA Interaction, Cancer Diagnosis, Nanotechnology

1 Introduction

Nanoparticles are considered to be engineered materials having dimensions in the size range of 1 to 100nm in diameter. Biological structures and molecules have matching size range as that of nanoparticles such as DNA, viruses and proteins. Hence nanomaterials are mainly best suitable for the applications including biological interactions, for example, biosensing and therapeutics. To date large number of diverse nanoparticles has been well-defined in literature. In comparison to bulk materials most of the atoms in nanoparticles are found on their surface. Taking example of a 1cm cube of iron, only 0.00001% of its atoms are sited on the surface while in contrast for 10nm or 1 nm cubes the value increases to 10% and 100%, respectively [1]. This atomic arrangement in nanoparticles leads to a number of properties different to their respective bulk material. Quantum effects arises due to size reduction and atomic confinement, this results in distinctive physicochemical properties, such as surface plasmon resonance, narrow wavelength fluorescence, super paramagnetic, or ultrahigh absorbance that cannot be realized with bulk materials.

Moreover, nanoparticles exhibit extraordinary surface-to-volume ratio which allows almost all surfaces to be open for bio interactions and chemical functionalization for a given amount of material. As the size of the nanoparticle increases, surface-to-volume ratio also changes quickly to evident size-dependent effects, such as shifting of the absorption wavelength of AuNPs.

Irradiating these particles with light of particular frequency applies a force on the conduction band electrons, which displaces them to one side of the surface of the particle. A dipole is formed from this charge difference inside the particle. Strong electromagnetic field amplification is caused by the dipole that can resonate with the incident light photon oscillations. This practice as the most famous optical effect of nanoparticles called as surface plasmon resonance. The surface area along-with the distance between the positive and negative charges of the dipole defines the resonance wavelength for SPR. Hence, nanoparticle size and shape are controlled by SPR spectral maximum. The SPR maximum wavelength can also be influenced due to the surface chemistry and ligand functionalization. SPR can significantly enhance the extinction cross section of the nanoparticle upto 10 times greater than its real cross section. So this amazing plasmonic effect of nanoparticles makes them the ideal contrast nominees for colorimetry.

Gold nanoparticles structure considered as an ionic lattice with electrons confined within conduction band but have free movement through the nanoparticles surface [2]. AuNPs have been famous due to their physical, chemical and optical properties including surface plasmon resonance which are different from their bulk material. They can be synthesized by variety of chemical, physical and green methods. These particles show strong affinity for DNA due to large surface bio conjugation available for molecular probes. These label-free gold nanoparticles used as biosensors mainly rely on the SPR shifts induced by the refractive index changes. In correspondence to their plasmonic properties, AuNPs are biocompatible and can be easily treated for functionalizing their surface with the requisite ligands. This is realized simply by mixing AuNPs with the ligand of concern (such as nucleic acid) that has been modified with a suitable functionality. Negatively charged functional groups like DNA will also show weak electrostatic interactions with the AuNPs, however, upon removal of these charged groups, stability of the AuNPs are disrupted and aggregation can happen [3]. Moreover, the variability of these materials are further demonstrated by the diversity of ligands that are capable of stabilizing AuNPs such as citrate, phosphine, phosphine oxides, thiols, amines and carboxylates.

Finding colorimetric reporters, like AuNPs sensors, in the early detection and monitoring of diseases has proven to be of utmost importance in reducing the impact and improving the survival rate in patients. One of the main attributes of diagnostic tests designed for a clinical setting is the accuracy and sensitivity of the assay. However, due to high processing times, sophisticated instrumentation and lack of skilled worker, such options are often not available in developing countries.

AuNPs are the most commonly used and most popular, due to their stability in solid or solution form [4], also they are easily conjugated and are relatively inert [5]. Furthermore AuNPs immunoassays

are often more sensitive [6]. For example, Liu and coworkers have demonstrated the feasibility of detecting influenza A in an optimized aggregation based system in 30 minutes without the requirement of instrumentation or enzymes. It was found out that nucleotide bases of single and double-stranded molecules possess diverse concentrations to adsorb onto AuNPs in colloidal solutions [7]. The AuNPs with diverse sizes and shapes comprising of nanospheres, nanobranches, nanocubes and nanorods were studied. The efficiency of this system found to be dependent on the shape and the size of the AuNPs. Even more recently, amplification based methods using human serum analysis for cardiac troponin I has been demonstrated with silver staining of bound Ab-AuNPs in a sandwich assay with a turnaround time of 1.5 hours compared to traditional ELISA of 3 hours [8]. While the analysis of human biological samples still rely on ELISA, the transition towards AuNPs as a reporter has been well documented in screening studies [9]. Although antibodies are still the gold standard of recognition (probe) materials, replacement with aptamers, a nucleic acid analogue of antibodies, has been foreseen to have inherent advantages over antibodies [10].

As stated, one of the most marvelous properties of AuNPs is their ability to reversibly aggregate and disperse leading to colorimetric changes [11]. The stability of functionalized AuNPs is due to the capping ligand that is surrounding the AuNPs shell, which affects the surface potential [12]. By increasing the potential, the capping ligand limits inter-particle interactions and prevents aggregation. Single-stranded DNA is an excellent stabilizer and avoids the aggregation of AuNPs due to its highly negative charge. DNA with the deoxyribose-phosphate backbone interacts with AuNPs through electrostatic interaction [7]. AuNPs mediated biological assays are preferable over traditional fluorescent or radiolabeled assays due to the basic characteristics of facile synthesis and biocompatibility of AuNPs [13]. The key advantage of using AuNPs solution as an assay is that the detection of biomolecules as color change of the solution is possible through naked eye [14]. Due to very high extinction absorption coefficients of AuNPs, AuNPs-DNA assay offers high sensitivity. The earliest utilization of DNA functionalized AuNPs as a colorimetric platform was reported in 1996 when the Mirkin group successfully functionalized AuNPs with thiolated DNA in a way that exhibited unusual melting and optical properties. In their study, AuNPs were synthesized using citrate capped 13 nm AuNPs and incubated with thiolated DNA. The sequence of DNA base pairs defines their role during which gene expression is as important [15] as transcription and replication. Genetic expressions are reprogrammed in case of cancers, which generates a special methylation pattern as well as assembled methylation landscapes at regions of DNA.

The main idea of conducting this project is to find out an easy, non-invasive, cheap and fast method of cancer detection by using colorimetric and UV/Vis spectral shift response of DNA mediated AuNPs assemblies.

The research work presented here is a step towards easy, robust and low cost diagnosis of breast cancer in less time as compared to other techniques. Although this work has a good potential to detect cancer at an early stage. This study presents an open area which should be very helpful to generalize the results by increasing the sample size. Though current research work is well performed with very promising results with each sample performed in triplicates but one limitation was with low sample size.

This principal characteristic of color transformation from red to blue owing to aggregated and non-aggregated ways in AuNPs had read the cancer through colorimetric examination and SPR (surface plasmon resonance) peak shift. Colorimetry has several advantages for biosensing applications. However, this method relies on the UV/Vis readout to detect tumor occurrence. The main focus of this study was to showcase applications of AuNPs in colorimetric and spectroscopic diagnostic applications.

2 Material and methods

This section will discuss the methodology of DNA extraction through blood and characterization with a brief introduction to synthesis of AuNPs, accompanied by the technique to study the change in optical properties of AuNPs-DNA as color of colloidal AuNPs and SPR peak of UV/Vis spectrum is

size dependent. DNA Extraction has been done from whole blood samples of Cancer patients and normal controls. All Spectroscopic information regarding nanoparticle peak wavelength and absorbance, DNA and nanoparticle interaction mediated plasmon peak shift was recorded by UV/Vis spectrophotometer of Spectroscopy Lab of Physics Department of UAF.

2.1 Chemical Equipment

The following materials have been purchased from Sigma Aldrich: tetrachloroauric acid molecular weight 339.775, trisodium citrate dehydrate molecular weight 258.06, HCl and NaCl were used. The double distilled deionized water used for all reactions and synthesis processes. Everything used in glassware in these experimental carefully washed thrice in aqua regia (HCl:HNO3) in 3:1 ratio, and then further bathed with ethanol followed by air drying.
Thermo Scientific Whole Blood Genomic DNA Purification Kit #K0781, #K0782 was purchased for DNA Extraction from whole blood samples of Cancer patients and normal controls. The standard protocol for DNA extraction by this kit is attacthed in supplementary material. Nanodrop 1000 was used from CABB, UAF, to quantify of DNA concentrations after DNA extraction. All Spectroscopic information regarding nanoparticle peak wavelength and absorbance, DNA and nanoparticle interaction mediated plasmon peak shift was recorded by UV/Vis spectrophotometer of Spectroscopy Lab of Physics Department of UAF.

2.2 Protocol to Prepare 5SSC Buffer

1M Saline Sodium Citrate buffer utilized in this work for AuNP-DNA solution phase probing was prepared by taking 3M NaCl (molecular weight 58.44) with 0.3M sodium citrate (molecular weight 258.06). The detail steps to prepare buffer are attached in supplementary data.

2.3 Blood Samples

24 blood samples with histologically confirmed cases (some patient's reports are attached in supplementary section as proof) from different cancer patients were collected from PINUM CANCER Hospital, Faisalabad, along-with 12 disease-free individuals forming the independent set according to statistical model and the details of the model is attached in supplementary material.

2.3.1 Informed Consent from patients

The relevant ethical approval was obtained from Director PINUM CANCER HOSPITTAL, Faisalabad for blood collection and also from the ORIC University of Agriculture Faisalabad for all blood samples analysis presented in this study. All samples were collected in a tube manifested with a number in a blinded fashion with informed consent by patients and healthy individuals.

2.4 DNA Characterization

DNA extracted from blood was analyzed for concentration by Nanodrop UV/Vis absorbance monitoring at 260 nm. The details of each DNA concentration is attached in supplementary data set.
2.5 Synthesis and characterization of AuNPs
Gold (III) chloride hydrate, HAuCl4.3H2O was reduced by citrate to produce AuNPs in colloidal solution form agreeing and extending from the subsequent technique established on the famous Turkevich method [16], [12], as shown in **Table 1**. The requisite volume containing dissolved salt solution of HAuCl4.3H2O was heated on magnetic stirrer at maximum speed to the boiling point whereas the solution kept stirring vigorously and at this point trisodium citrate was added rapidly.

The color of the solution shifts from pale yellow to deep violet first within 10 minutes, next it changes slowly to deep red as an indication that the nanoparticles are formed, as shown below (see Figure 1). The solution kept boiling for different periods of time to guarantee that the reaction is completed and to produce stable size nanoparticle while their details about size and shape are further elaborated in result and discussion set.

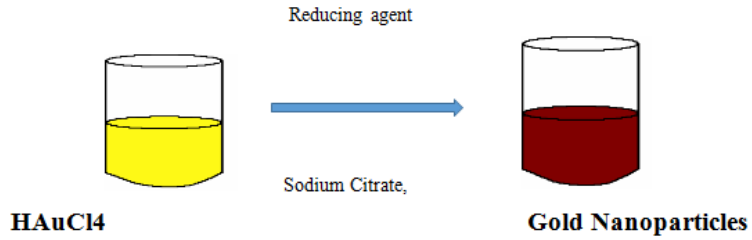

Figure 1. Schematic representation of chemically synthesized Gold nanoparticles

Table 1: Experimental conditions and the concentrations on the reactant used for the synthesis of AuNPs capped by citrate

Sample code	HAuCl4 ml /(mM)	trisodium citrate (mM)	Temperature (0C)	Reaction Time Hr	Reference
S1	50 ml 1 mM	5 ml 40 mM	100	3 hr	[12] [17]
S2	125 ml .25 mM	12.5 ml 40 mM	100	2 hr	
	20ml 0.25 mM	2 ml 40 mM			[18]
S3	100 ml 1 mM		100	30 min	
		4 ml 38.8 mM			[16]
S4			100	3 hr	

This principal characteristic of color transformation from red to blue owing to aggregated and non-aggregated structures AuNPs had read the tumor through colorimetric examination and SPR (surface plasmon resonance) peak shift. Colorimetry has several advantages for biosensing applications. However, this method relies on the UV/Vis readout to detect tumor occurrence. The main focus of this study was to showcase applications of AuNPs in colorimetric and spectroscopic diagnostic applications.

2.5.1 Spectroscopic Measurements

UV/Vis studies were carried out to characterize these citrate capped AuNPs with and without salt incorporation. Absorption spectra (350 to 900nm) of sole AuNPs and AuNPs + DNA (Cancer and Normal) samples with added salt were analyzed using UV/Vis 6800 spectrophotometer.

2.5.2 Microscopic Measurement

AuNPs with and without salt were characterized for mean size and size distribution studies by TEM and AFM. Imaging was done on a Hitachi H8000 Scanning Transmission Electron Microscope at 200 kV accelerating voltage. The TEM used imaging mode by standard samples and was calibrated for diffraction.

2.5.3 AuNP size measurement with dynamic light scattering

The size of synthesized AuNPs was measured using dynamic light scattering. The nanosizer software controls the instrument and permits to analyze the data to either drive the size or the zeta potential information of the particles.

2.5.4 Imaging AuNPs with Transmission Electron Microscopy (TEM) and Atomic Force Microscopy TEM and AFM which has a resolution of up to 0.45nm and 0.1nm respectively were used to visualize both the AuNPs alone and with salt to check for aggregation. It produces bright dark field images. Average particle size, shape were calculated from the observation of at least 100 particles.

2.6 Colorimetric Nanoparticles based DNA Analysis

AuNPs exhibit sharp color diversity in disperse and aggregated form [19], [20]. DNA and AuNPs affinity is well known from literature [4], experiments are performed using citrate capped AuNPs of sample S2, which were then mixed and incubated for 5 minutes with genomic DNA extracted from 24 cancer patients and 12 normal individuals, followed by the addition of the prepared 5SSC buffer, the relevant amount of all the entities used are listed in the tables. UV/Vis spectrophotometer is utilized to record the absorbance profiles versus wavelength for all the AuNPs-DNA samples. One interesting feature of this study is that nanoparticles SPR peak remained stable in 19 cancer samples out of 24 as there was no plasmon peak shift in them and solution color remained red showing no AuNPs aggregation, while healthy sample mixtures distinctively shifted their plasmon peak to longer wavelengths (red shift) which was visible to naked eye as blue color which clearly showed that AuNPs become aggregated.

3 Result and Discussion

The transition states of AuNPs from dispersion to aggregation upon salt addition induce color change from pink to blue observed by the naked eyes in their colloidal solution;[21] also this change of state can be examined with the help of various UV/Vis absorption spectra, together with the corresponding surface plasmon resonance peak shift in the ultraviolet/visible spectrophotometry (UV/Vis) [22]. Consequently, we have planned this novel research demonstrating the curious difference between DNA from cancer and healthy individuals on the behalf of AuNPs and DNA affinity interactions [4]. This DNA mediated AuNPs affinity response appeared to be common in all cancer DNAs, which is clearly different from normal DNAs, observed as color change and resonance peak shift using 40nm chemically synthesized citrate-capped AuNPs. The color of the colloidal solution of AuNPs changes depending upon if cancer DNA is present or not, in a very short interval of time. So due to its simplicity and robustness, this AuNPs-DNA affinity response could become a universal blood test for cancer detection. Based on this potential response, AuNPs are proved be effective biomarker for colorimetric detection of Cancer. Additionally, AuNPs must stay stable in vitro environment that imitates in vivo situation for any potential biomedical applications. A lot of research has been done that relate results from different AuNPs size dependent colorimetric and SPR peak shift response, (with mean size up to 80nm or above) conjugated to genomic DNA (with no PCR performed on it) to detect cancer.

3.1 Synthesis of AuNPs

In this work, synthesis of AuNPs with different sizes was carried out using citrate as capping agent. Different molar concentrations of HAuCl4.3H2O was reduced by varying the amount of sodium citrate tribasic dehydrate to produce different sized AuNPs with sample codes S1, S2, S3 and S4 (Table 1), solution color varies from pale yellow to grey and then to red confirming that spherical monodispersed gold nanoparticles [23] have been formed, see Fig *2*. It was observed that apart from using different molar concentrations of gold solution and sodium citrate, temperature and time duration of reaction are also important factors in regulating the size of AuNPs.

Fig 2. Color of bulk gold solution changed from pale yellow to ruby red upon AuNPs formation

3.1.1 Dynamic Light Scattering measured hydrodynamic sizes

DLS measurement computed the hydrodynamic diameter which includes core size of the particles along-with size of the coating agents. The z-average values measured with DLS for citrate stabilized AuNPs samples S1, S2, S3 and S4 vary from 35 nm to 50 nm respectively. DLS graphs presented below (Fig 3) demonstrates that synthesized samples have dissimilar sizes.

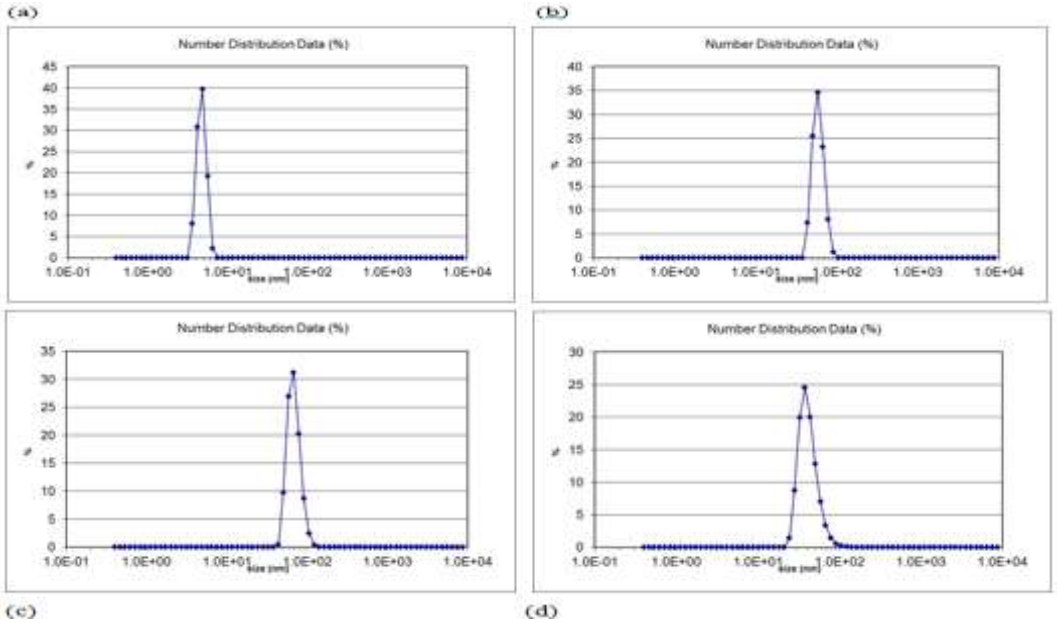

Fig 3. DLS diagrams of four AuNPs samples demonstrating the sizes of the particles. Samples (a) S1. (b) S2, (c) S3 and (d) S4 are stabilized by citrate. For the sample S4 in figure (d) shows the peaks around 100nm which corresponds to large sized AuNPs.

3.1.2 TEM and AFM calculated core sizes of AuNPs

TEM and AFM micrographs of synthesized AuNPs before and after adding salt were measured using TEM and AFM. The micrographs of representative sample S2 are presented below (Fig. 4) i.e., for 40nm citrate capped AuNPs. The mean core sizes of citrate capped AuNPs from at least 100 particles are in the range of 32.6 nm to 40 nm of sample S2.

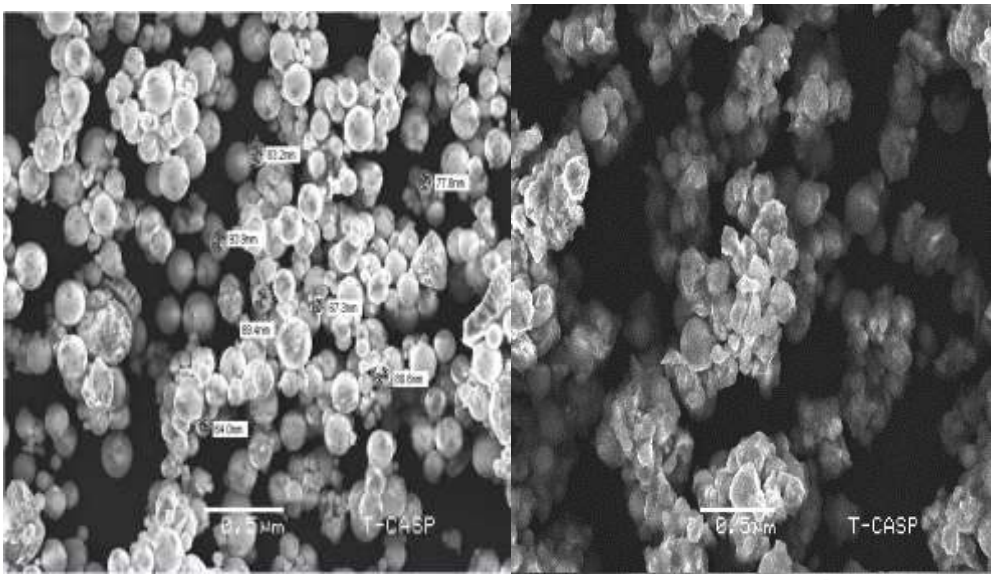

(a) (b)

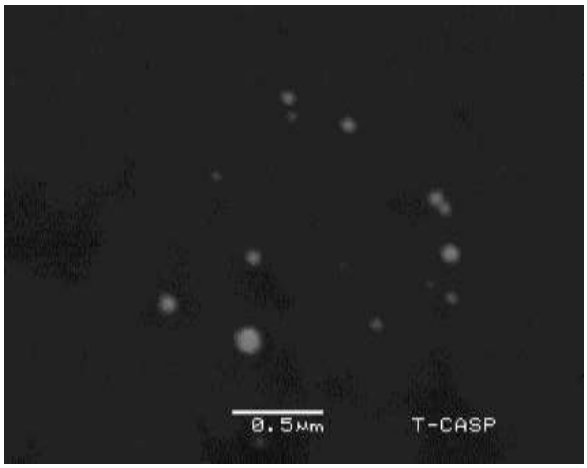

(c)

Fig. 4: TEM image of citrate capped AuNPs of sample S2 (a) before salt addition (b) after salt addition (c) AFM image of 40nm citrate capped sole AuNPs of sample S2.

The difference in size from DLS and TEM measurement can be due to the factors including polydispersity may be and the type and size of coating agent. Also TEM measures the sizes of core of the particles while DLS calculates the hydrodynamic diameter of particles. So DLS gives the size including the core the coating agent and any associated water, so we can rely more on TEM measurements rather than DLS.

3.2 Shapes of AuNPs

TEM micrographs of freshly synthesized AuNPs are presented above see Fig. 4 (a), they have revealed clearly the spherical shapes of the synthesized nanoparticles. These graphs clearly show the occurrence of spherical nanoparticles.

3.3 Stability of AuNPs

AuNPs sample S2 stability with SPR peak at 536 was recorded and monitored solely and in different DNA environments using UV/Vis spectroscopy. The characteristic absorption peak was analyzed for a good 7 day period and was further monitored for the aggregation of AuNPs; these particles must be stabilized by some appropriate coating agents to avoid aggregation. Lacking a suitable stabilizing agent will source the reason of constant growing of these particles and hence aggregation of the AuNPs. In our work, stability of AuNPs has been routinely checked over a period of five months since the time of their preparation before mixing with DNA in each reaction. The SPR spectra of these samples, especially S2, were recorded for a period of five months using UV/Vis spectrometer. Results discussed here exhibited stability of the SPR peak over 4 months period with negligible change (as size change <10nm is acceptable) in size but if we observe (Fig. *5*) closely then it is clear that after a month of preparation AuNPs bandwidth become little larger than the day AuNPs were synthesized which can be regarded as particle agglomeration and after 5 months peak become more broad and color conversion of AuNPs from ruby red to purple had clearly showed that size of original AuNPs has been increased from 40 nm as SPR wavelength is red shifted in the five months duration of study as shown in (d) (e)

Figure 12 (d), *(*d) (e)

Fig. 13 (e)]. So in current dissertation, we have used these high-quality, stable AuNPs to study their effect/interaction with normal and cancerous DNA for cancer detection.

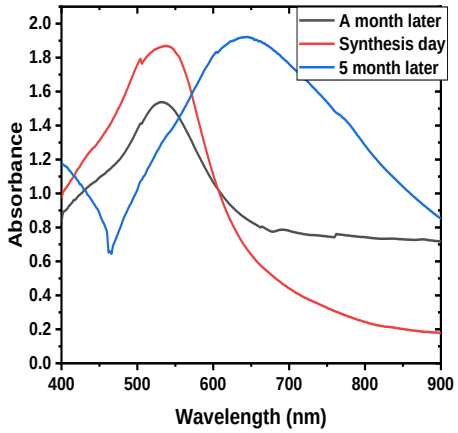

Fig. 5: SPR spectrum of citrate stabilized AuNPs from sample S2 showing the stability with approximate size of 40nm over a period of 4 to 5 months.

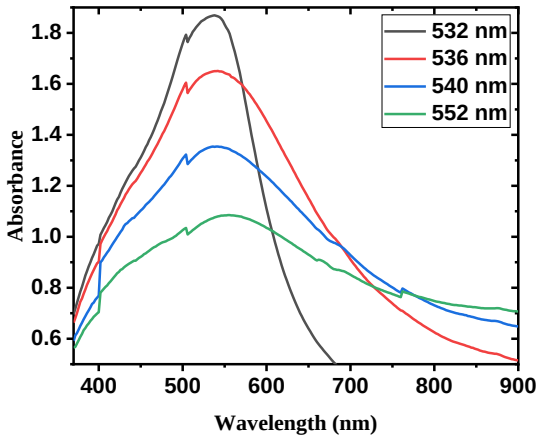

Fig. 6: The UV/Vis absorption Spectra of freshly prepared AuNPs of samples S1, S2, S3 and S4.

3.4 Colorimetric Response of AuNPs-DNA Interaction upon salt addition

The overall strategy of the novel method of Colorimetric Response by citrate capped 40nm AuNPs and DNA Interaction is illustrated below;

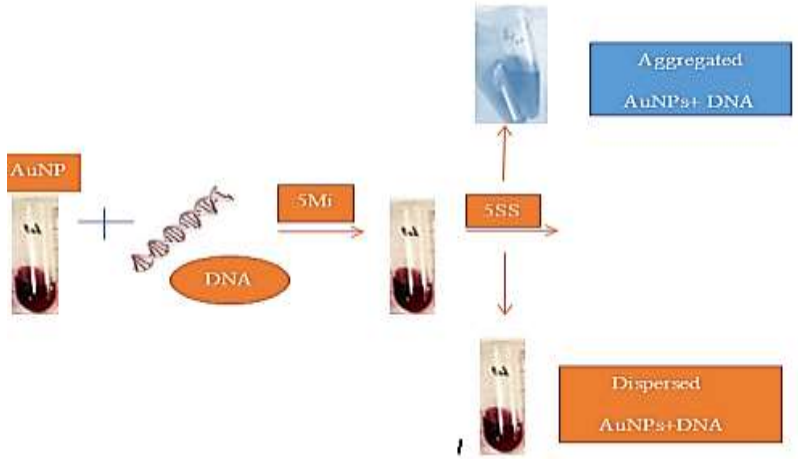

Fig. 7. Schematic Diagram of Overall Strategy of Cancer detection via AuNPs and DNA interaction.

AuNPs [24] are widely used as biomarker for DNA detection because of their extraordinary optical properties [25]. Along-with optical properties, AuNPs colorimetric response proved to be an effective biomarker for detecting any anamoly in DNA [3]. Noble metal nanoparticles have size, shape, concentration and aggregation state dependent optical properties [26]. Here in this research work, we have highlighted this novel observation of transformation of ruby red, monodispersed 40nm citrate capped AuNPs to purple color agglomerated AuNPs colloidal solution over a period of 5 months characterized by UV/Vis spectrophotometer where their SPR peak shifts from 536nm to 546nm ((d) (e)

Figure 12, (d) (e)

Fig. 13), which is still considered stable under the mentioned criteria for a change is acceptable if <10nm. As polydispersity is characterized by size non uniformity of nanoparticles, here in this research work it is observed that ((d) (e)

Figure 12, (d) (e)

Fig. 13) AuNPs become polydisperse due to particle agglomeration as electrostatic repulsions are overruled after long time of their preparation as citrate is not a very good stabilizing agent verifying the fact that Turkevich method is suitable only for small size particle synthesis upto 40-50nm. In (d) (e)

Fig. 13, this polydispersity character has become evident for cancer samples (20-24) as the colloidal solution containing AuNPs appeared purple color ((d) (e)

Fig. 13) instead of red with shifted plasmon peak to 550nm or higher, but these polydispersed AuNPs still showed the potential to effectively differentiate normal genomic DNA from cancer ones as sharp grey to blue color as shown in (d) (e)

Fig. 13 (c-d).
It has been analyzed that the absorption peak wavelength increases with the increase of size of AuNPs. This absorption maximum peak is shifted to a wavelength of 560nm (650nm in case of blue) when particles size got increased due to agglomeration (120nm). This induces red shift of plasmon peak which is a mark of increased particle size of AuNPs ((d) (e)

Figure 12, (d) (e)

Fig. 13). The position of maximum peak of polydispersed purple color AuNPs does not really provide any information about the size of AuNPs, since peak separation is not possible from specific populations in colloidal solution [26].

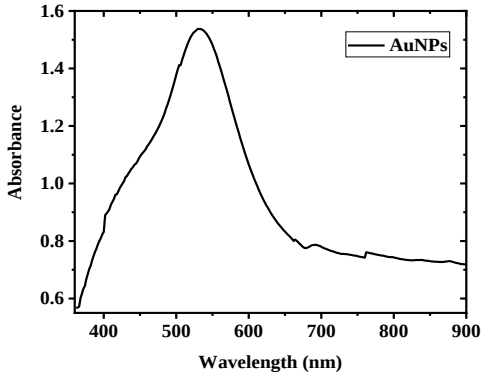

Fig. 8. UV/Vis spectrum of chemically synthesized citrate capped AuNPs alone with SPR peak at 536nm.

DNA mediated colorimetric response of AuNPs had proven the efficacy of this study as shown in five different probes with 40 nm citrate capped AuNPs (Fig. 9-(d) (e)

Fig. 13). 40nm citrate-capped AuNPs mediated DNA probes were fabricated to diagnose cancer from normal samples which is utterly based on SPR trait of AuNPs colloidal solution [3]. The stability and sensitivity of these probes are verified by in-vitro AuNPs-DNA mediated response as color change and SPR peak wavelength shift. The results showed that the AuNPs-DNA aggregation and non-aggregation states upon salt addition were with the capacity to diagnose cancerous DNA from healthy ones.
In the IST probe, DNA samples 10 and 12 of cancer patients and DNA 10 from normal person have been analyzed for colorimetry response. The color remained red for cancerous DNA samples 10 and 12 and a clear blue color is observed for normal DNA sample 10 confirming particle aggregation upon salt addition by SPR peak shift with large broadening in their UV/Vis absorption spectrum while for cancerous samples the SPR peak stayed stable at 536 nm with narrow band width showing no particle aggregation (Fig. 9*)*. The color of cancerous AuNPs solutions remained red even after salt addition in 19 samples out of 24 and turned blue in respective normal DNA probes. The experimental details of the volume and concentration of all the probes are given below (Table 2-

Table 6) for 1M saline 5SSC buffer. DNA Concentration is stabilized to 50 ng/ul by adjusting DNA volume.

Table 2: First Experiment for 1X solution of AuNPs and DNA interaction.

Sr.No	DNA Sample	DNA Conc. ng/µl	DNA Vol (1X) ng/µl	AuNPs Vol (1X) µl	5SSC Salt Vol (1X) µl	Result Pink/Blue
1	10	31.8	1.6	25.5	4.5	Pink
2	12	22.0	2.3	25.5	4.5	Pink
3	10 (Normal)	382.2	1	25.5	4.5	Blue

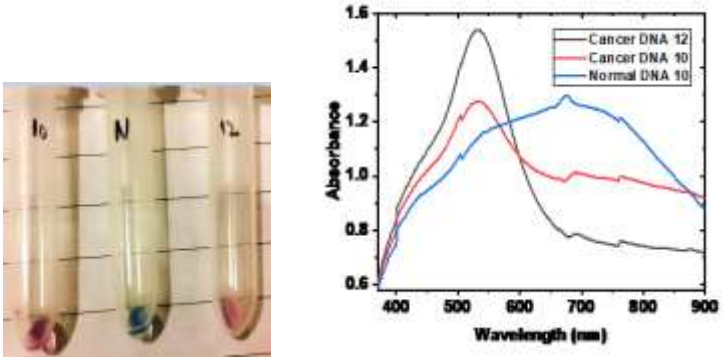

(a) (b)

Fig. 9. Naked eye detection of cancer using AuNPs for different DNA types (a) after salt addition (b) UV/Vis Spectrum of cancer and normal DNA.

In the second Probe, DNA samples (1, 2, 3, 4, 7) from cancer patients and DNA 2 of normal person have been analyzed for colorimetric response. The experimental details regarding AuNPs, DNA and salt solution for IX is shown below (

Table 3). It was observed that all cancer DNA samples stabilized AuNPs upon salt addition fairly by retaining the solution color as red except sample 4 which instantly turned blue when salt was added showing a broad spectrum shift towards longer wavelength of UV/Vis spectrum as shown below (Fig. 10). The color change can be clearly seen between normal and cancer samples upon salt addition and specifically the color of DNA sample 4 is clearly purple not pink indicating the aggregation of AuNPs (Fig. 10 b)

Table 3: 2nd experiment 1X solution of AuNPs and DNA interaction for colorimetric change upon salt addition

Sr.No	DNA Sample	DNA Conc. ng/µl	DNA Vol (1X) ng/µl	AuNPs Vol (1X) µl	5SSC Salt Vol (1X) µl	Result Pink/Blue
1	1	10.2	5	25.5	4.5	Pink
2	2	7.6	7	25.5	4.5	Pink
3	3	12.5	4	25.5	4.5	Pink
4	4	25.3	2	25.5	4.5	Blue
5	7	20.6	2.5	25.5	4.5	Pink

11	12 (Normal)	14.6	3.5	25.5	4.5	Blue

(a) (b)

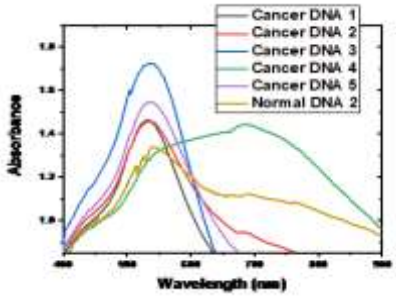

(c)

Fig. 10. Probe 2, Naked eye detection of cancer using AuNPs for different DNA types (a) before salt addition (b) after salt addition(c) UV/Vis Spectrum of cancer and normal DNA.

In the third Probe, DNA samples (5, 6, 8, 9, 11, 13) from cancer patients and DNA 4 from normal person have been analyzed for colorimetric response. The experimental details regarding AuNPs, DNA and salt solution for IX can be seen in (

Table ***4***). It was observed that all cancer DNA samples stabilized AuNPs upon salt addition fairly retaining the solution color as red except sample 5, 8 and 13 which instantly turned purple when salt was added showing a broad spectrum shoulder shift towards longer wavelength of UV/Vis spectrum as shown below (Fig. 11 b,c,d), but as the change in SPR peak wavelength <10nm so according to above mentioned criteria this Probe is considered stable for this specific time of observation with some particle aggregation due to change in size of nanoparticles or surrounding environment.

Table 4: 3rd Experiment with 1X solution of AuNPs and DNA interaction.

Sr.No	**DNA Sample**	**DNA Conc. ng/µl**	**DNA Vol (1X) ng/µl**	**AuNPs Vol (1X) µl**	**5SSC Salt Vol (1X) µl**	**Result Pink/Blue**
1	5	50.3	1	25.5	4.5	Blue
2	6	14.9	3.4	25.5	4.5	Pink
3	8	56.4	1	25.5	4.5	Pink
4	9	7.4	6.8	25.5	4.5	Pink
5	11	34.5	1.5	25.5	4.5	Pink
6	13	41.6	1.3	25.5	4.5	Pink
7	11 (Normal)	17.5	2.8	25.5	4.5	Blue

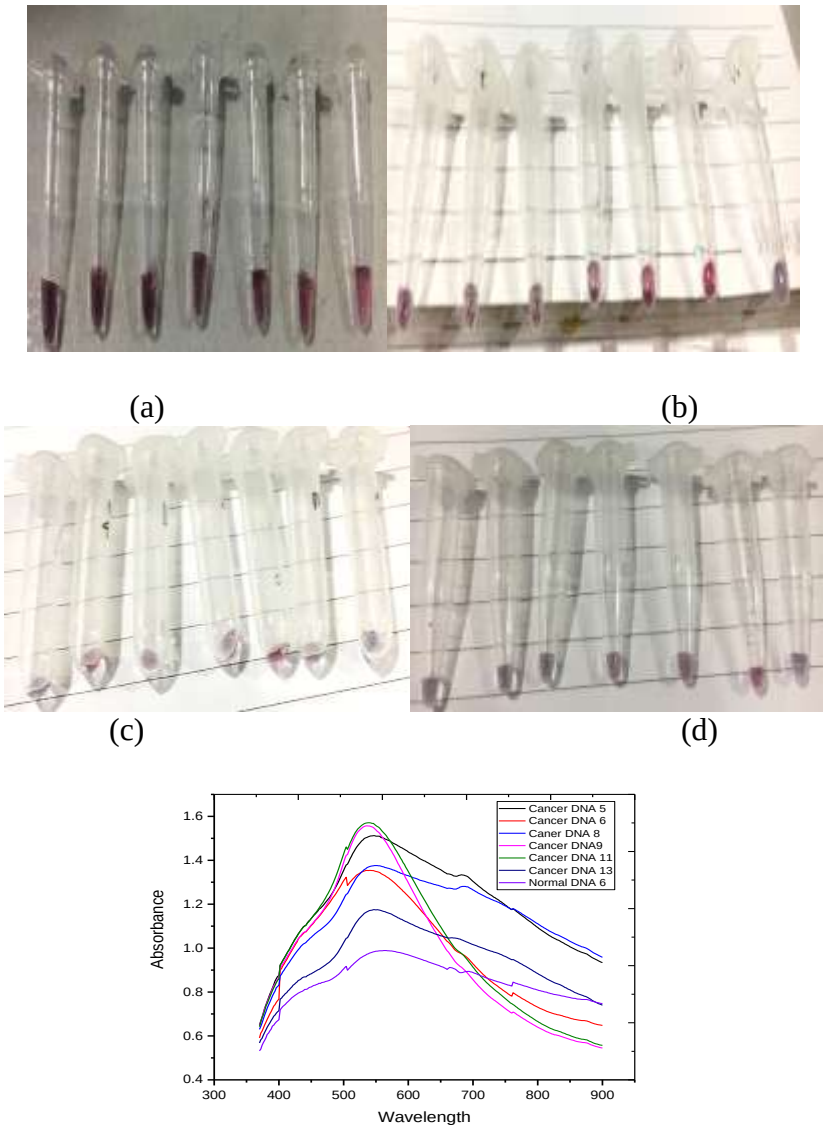

(e)

Fig. 11. Probe 3-Naked eye detection of cancer via aggregation based color change behavior of the AuNPs-DNA solution for different DNA types (a) before salt addition (b) after salt addition (c) repeated the same experiment with same samples, after salt addition (d) repeated again (e) UV/Vis Spectrum of AuNPs-cancer DNA samples and AuNPs-normal DNA

In the fourth Probe, DNA samples (14, 15, 16, 17, 18, 19) from cancer patients and DNA (1, 2, 3, and 4) from normal patient has been analyzed for colorimetric response. The experimental details regarding AuNPs, DNA and salt solution for IX is shown below (
Table 5). It was observed that cancer DNA samples which fairly retained the solution color as red are 16 and 17 and while sample 14, 15 and 18 and 19 showed a broad spectrum shoulder shift towards longer wavelength of UV/Vis spectrum as shown below ((d) (e)

Figure 12).

Table 5: 4th Experiment with 1X solution of AuNPs and DNA Interaction

Sr.No	**DNA Sample**	**DNA Conc. ng/µl**	**DNA Vol (1X)**	**AuNPs Vol (1X)**	**5SSC Salt Vol (1X)**	**Result Pink/Blue**

			ng/µl	**µl**	**µl**	
1	14	66.6	1	25.5	4.5	Blue
2	15	6.4	8	25.5	4.5	Pink
3	16	23.8	2.2	25.5	4.5	Pink
4	17	10.7	4.7	25.5	4.5	Pink
5	18	4.8	10.7	25.5	4.5	Pink
6	19	8.4	6	25.5	4.5	Pink
7	1 (Normal)	23.9	2.1	25.5	4.5	Blue
8	2 (Normal)	19.3	2.6	25.5	4.5	Blue
9	3 (Normal	13.1	3.9	25.5	4.5	Blue
10	4 (Normal)	12.5	4	25.5	4.5	Blue

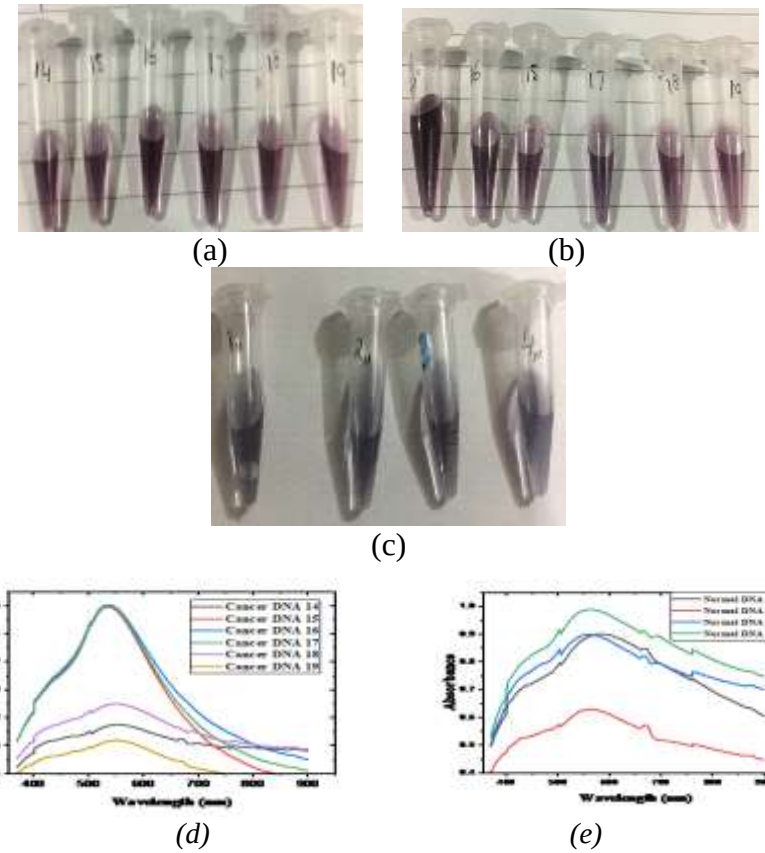

Figure 12: Probe 4-Naked eye detection of cancer via aggregation based color change behavior of the AuNPs-DNA solution for different DNA types (a) before salt addition (b) after salt addition (c) normal DNA samples after salt addition showing blue color (d) UV/Vi s Spectrum of AuNPs-cancer DNA samples (e) UV/Vi s Spectrum of AuNPs-normal DNA samples.

In the fifth Probe, DNA samples (20, 21, 22, 23, 24) from cancer patients and DNA (5, 6, 7, 8) from normal patient has been analyzed for colorimetric response. The experimental details regarding AuNPs, DNA and salt solution for IX and 25X volume are shown below (

Table **6**) respectively. It was observed that cancer DNA samples which fairly retained the solution color as red are 23 while rest samples showed little to moderate aggregation, as obvious from the color of the solution after salt addition, in the ignorable limit where we considered the AuNPs stable as change in wavelength shift is <10nm from 546nm to 554nm or less. So sample 20, 21, 22 and 24 showed a broad absorption spectrum with a shoulder shift towards longer wavelength of UV/Vis spectrum as shown in ((d) (e)

Fig. 13).

Table 6: 5th Experiment with 1X solution of AuNPs and DNA interaction

Sr.No	DNA Sample	DNA Conc. ng/µl	DNA Vol (1X) ng/µl	AuNPs Vol (1X) µl	5SSC Salt Vol (1X) µl	Result Pink/Blue
1	20	8.6	5.8	25.5	4.5	Pink
2	21	17.3	3	25.5	4.5	Pink
3	22	7.6	6.6	25.5	4.5	Pink
4	23	5.3	9.5	25.5	4.5	Pink
5	24	16.1	3.2	25.5	4.5	Pink
6	5 (Normal)	8	6.3	25.5	4.5	Blue
7	6 (Normal	15.1	3.4	25.5	4.5	Blue
8	7 (Normal)	7.6	6.6	25.5	4.5	Blue
9	8 (Normal)	8.2	6.1	25.5	4.5	Blue

(a) (b)

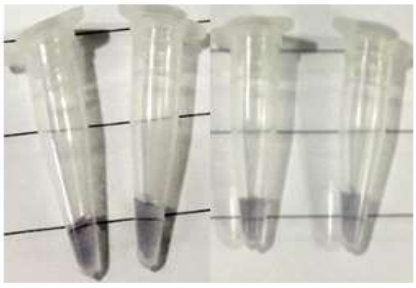

(c)

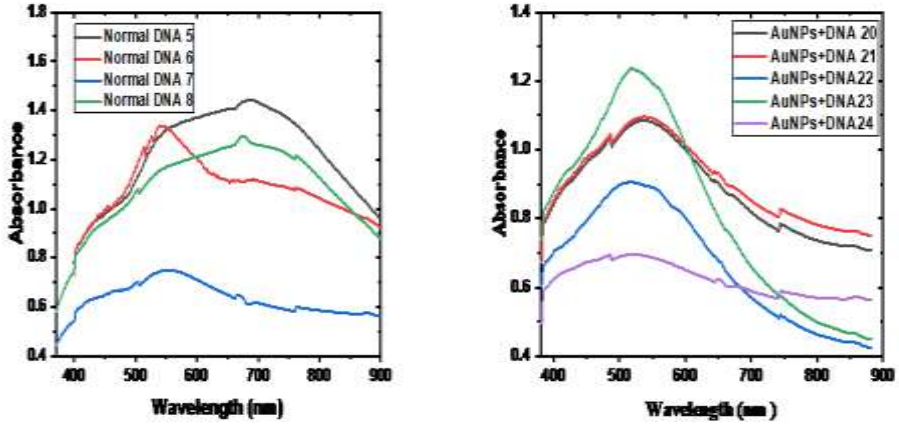

(d) *(e)*

Fig. 13. Probe 5-Naked eye detection of cancer via aggregation based color change behavior of the AuNPs-DNA solution for different DNA types (a) cancer samples before salt addition (b) after salt addition (c) normal DNA samples after salt addition showing blue color s (d) UV/Vis Spectrum of AuNPs-normal DNA samples (e) UV/Vis Spectrum of AuNPs-cancer DNA samples.

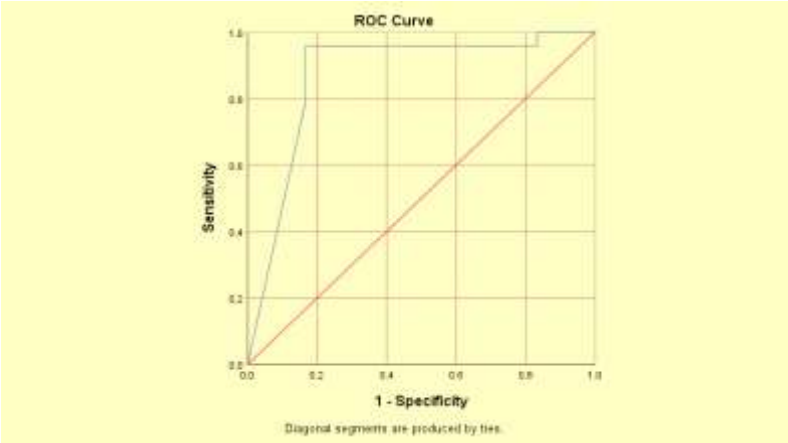

(a)

Test Result Variable(s): Test_Result

Area	Std. Error[a]	Asymptotic Sig.[b]	Asymptotic 95% Confidence Interval	
			Lower Bound	Upper Bound
.872	.075	.000	.724	1.000

(b)

Fig. 14. (a)The ROC analysis and diagnostic test evaluation shows area under the curve and (b) accuracy of the method

This methodology has exposed enormous prospective to diagnose cancer as proved by the ROC graphs (Fig. 14) of AuNPs mediated DNA solution where DNA is extracted from cancer and normal tissues. Also, this methodology has facilitated cancer detection through blood derived DNA test in a very short period of time of less than 10minutes with excellent specificity (e.g., AUC = 0.872 with visual detection of cancer with AuNPs). We consider that this modest methodology with outstanding sensitivity and specificity would theoretically be a superior substitute to the existing practices for cancer detection. Though, "AuNPs as a biomarker of cancer" in its present practice is only capable of determining the existence of disease. The comprehensive examination is mandatory to entirely grasp the stage, disease recurrence and type.

4 Conclusion

We had fabricated a 40nm citrate-capped AuNPs mediated DNA probe to diagnose cancer from normal samples which is utterly based on SPR trait of AuNPs colloidal solution [3]. The stability and sensitivity of the probe is verified by in-vitro AuNPs-DNA mediated response as color change and SPR peak wavelength shift. The results showed that the AuNPs-DNA aggregation and non-aggregation states upon salt addition were with the capacity to diagnose cancer whole genome DNA from healthy ones. This probe has numerous advantages as it provides a simple, cheap and fast way which has been utilized to detect breast cancer.

DNA mediated colorimetric response of AuNPs had proven the efficacy of this study as shown in five different probes with big size 40 nm citrate capped AuNPs (Fig. 9-(d) (e)

Fig. 13). The color of cancerous AuNPs solutions remained red even after salt addition in 19 samples out of 24. One strange or novel speculation of this colorimetric response is that we have observed a clear change in color of original AuNPs after 4 months of their preparation i.e., they showed up of purple color with λmax=544 and a broader spectrum showing particle aggregation. When we have performed the experiment for probe 4 and 5 using these purple color AuNPs, probes still maintained the purple color after salt addition with λmax slightly shifted and flatter towards the red end of UV/Vis spectrum in the ignorable range, and while comparing the color of probe with healthy DNA samples ((d) (e)

Fig. 13 c) a distinct grey to blue color confirmed that particles are aggregated as observed from UV/Vis spectrum ((d) (e)

*Fig. 13*e). So these colorimetric assays hold great potential to diagnose cancer. The characteristic SPR peak arises as a qualitative measure of size and monodispersity of particles. So here broadening may corresponded to polydispersity of the particles. The detailed study on the properties of gold nanoparticles had helped us to recognize and determine the AuNPs and DNA characteristic response relationship. It is again well established that the electrostatic interaction of negatively charged phosphate backbone of DNA and highly polarizable electron density clouds of AuNPs contribute to the stability of colloidal suspension of AuNPs against aggregation. In this research work, the stability of colloidal AuNPs-DNA conjugate is studied by DNA adsorbed efficiency, as colloidal AuNPs are hydrophobic in nature and DNA from cancer genome has heterogeneous cluster methylation pattern at promotor region forming the genome highly hydrophobic, so indeed these forces have played their part majorly in aggregation process.

Furthermore this methodology has exposed enormous prospective to diagnose cancer as proved by the ROC graphs of AuNPs mediated DNA solution where DNA is extracted from cancer and normal tissues. Also this methodology has facilitated cancer detection through blood derived DNA test in a very short period of time of less than 10minutes with excellent specificity (e.g., AUC = 0.872 with visual detection of cancer with AuNPs). We consider that this modest methodology with outstanding sensitivity and specificity would theoretically be a superior substitute to the existing practices for cancer detection. Though, "AuNPs as a biomarker of cancer" in its present practice is only capable of determining the existence of disease. The comprehensive examination is mandatory to entirely grasp the stage, disease recurrence and type.

Funding

This research did not receive any specific grant from funding agencies in the public, commercial, or not-for-profit sectors.

Acknowledgement

Our special thanks and gratitude to PINUM CANCER HOSPITAL, Faisalabad, Laser Spectroscopy Lab UAF and Biochemistry Department UAF for their immense support.

Disclosure

The author declares no conflicts of interest.

Data availability

Data underlying the results presented in this paper are available in supplementary material.

References

1. S. Link and M. A. El-Sayed, *Shape and Size Dependence of Radiative, Non-Radiative and Photothermal Properties of Gold Nanocrystals* (2000), **19**(3).
2. V. Klimov, "Surface Plasmons," Nanoplasmonics 63–90 (2014).
3. F. Xia, X. Zuo, R. Yang, Y. Xiao, D. Kang, A. Vallée-Bélisle, X. Gong, J. D. Yuen, B. B. Y. Hsu, A. J. Heeger, and K. W. Plaxco, "Colorimetric detection of DNA, small molecules, proteins, and ions using unmodified gold nanoparticles and conjugated polyelectrolytes," Proc. Natl. Acad. Sci. U. S. A. **107**(24), 10837–10841 (2010).
4. C. C. Chang, C. P. Chen, T. H. Wu, C. H. Yang, C. W. Lin, and C. Y. Chen, "Gold nanoparticle-based colorimetric strategies for chemical and biological sensing applications," Nanomaterials **9**(6), 1–24 (2019).
5. L. De Sio, R. Caputo, U. Cataldi, and C. Umeton, "Broad band tuning of the plasmonic resonance of gold nanoparticles hosted in self-organized soft materials," J. Mater. Chem. **21**(47), 18967–18970 (2011).
6. H. Li and L. J. Rothberg, "Label-free colorimetric detection of specific sequences in genomic DNA amplified by the polymerase chain reaction," J. Am. Chem. Soc. **126**(35), 10958–10961 (2004).
7. H. Li and L. Rothberg, "Colorimetric detection of DNA sequences based on electrostatic interactions with unmodified gold nanoparticles," Proc. Natl. Acad. Sci. U. S. A. **101**(39), 14036–14039 (2004).
8. K. M. Koo, A. A. I. Sina, L. G. Carrascosa, M. J. A. Shiddiky, and M. Trau, "DNA-bare gold affinity interactions: Mechanism and applications in biosensing," Anal. Methods **7**(17), 7042–7054 (2015).
9. K. Sato, K. Hosokawa, and M. Maeda, "Rapid aggregation of gold nanoparticles induced by non-cross-linking DNA hybridization," J. Am. Chem. Soc. **125**(27), 8102–8103 (2003).
10. Y. Liu, N. Zhang, P. Li, L. Yu, S. Chen, Y. Zhang, Z. Jing, and W. Peng, "Low-cost localized surface plasmon resonance biosensing platform with a response enhancement for protein detection," Nanomaterials **9**(7), (2019).
11. I.-I. S. Lim, L. Wang, U. Chandrachud, S. Gal, and C.-J. Zhong, "Assembly/Disassembly of DNA-Au Nanoparticles: A Strategy of Intervention," Res. Lett. Nanotechnol. **2008**, 1–4 (2008).
12. K. Rahme, J. D. Holmes, K. Rahme, J. D. Holmes, G. Nanoparticles, K. Rahme, and J. D. Holmes, "Dekker Encyclopedia of Nanoscience and Nanotechnology , Third Edition Gold Nanoparticles : Synthesis , Characterization , and Bioconjugation Gold Nanoparticles : Synthesis , Characterization , and Bioconjugation," (September), (2015).
13. Y. Liu, M. K. Shipton, J. Ryan, E. D. Kaufman, S. Franzen, and D. L. Feldheim, "Synthesis, stability, and cellular internalization of gold nanoparticles containing mixed peptide-poly(ethylene glycol) monolayers," Anal. Chem. **79**(6), 2221–2229 (2007).
14. K. Chen, M. Zhang, Y. N. Chang, L. Xia, W. Gu, Y. Qin, J. Li, S. Cui, and G. Xing, "Utilizing Gold Nanoparticle Probes to Visually Detect DNA Methylation," Nanoscale Res. Lett. **11**(1), (2016).
15. A. A. I. Sina, L. G. Carrascosa, Z. Liang, Y. S. Grewal, A. Wardiana, M. J. A. Shiddiky, R. A. Gardiner, H. Samaratunga, M. K. Gandhi, R. J. Scott, D. Korbie, and M. Trau, "Epigenetically reprogrammed methylation landscape drives the DNA self-assembly and serves as a universal cancer biomarker," Nat. Commun. **9**(1), 1–13 (2018).
16. J. Dong, P. L. Carpinone, G. Pyrgiotakis, P. Demokritou, and B. M. Moudgil, "Synthesis of precision gold nanoparticles using Turkevich method," KONA Powder Part. J. **37**(August), 224–232 (2020).
17. C. Nanostructures, "Materials 2015 , 8 , 2849-2862;," 2849–2862 (2015).
18. M. Iqbal, G. Usanase, K. Oulmi, F. Aberkane, T. Bendaikha, H. Fessi, N. Zine, G. Agusti, E. S. Errachid, and A. Elaissari, "Preparation of gold nanoparticles and determination of their particles size via different methods," Mater. Res. Bull. **79**, 97–104 (2016).

19. H. Zakaria, W. S. Abdelaziz, and T. Youssef, "Effect of size, concentration, and type of spherical gold nanoparticles on heat evolution following laser irradiation using tissue-simulating phantoms," Lasers Med. Sci. **31**(4), 625–634 (2016).
20. V. Mody, R. Siwale, A. Singh, and H. Mody, "Introduction to metallic nanoparticles," J. Pharm. Bioallied Sci. **2**(4), 282 (2010).
21. J. Huang, Y. L. Liou, Y. N. Kang, Z. R. Tan, M. J. Peng, and H. H. Zhou, "Real-time colorimetric detection of DNA methylation of the PAX1 gene in cervical scrapings for cervical cancer screening with thiol-labeled PCR primers and gold nanoparticles," Int. J. Nanomedicine **11**, 5335–5347 (2016).
22. B. Nikoobakht, Z. L. Wang, and M. A. El-Sayed, "Self-assembly of gold nanorods," J. Phys. Chem. B **104**(36), 8635–8640 (2000).
23. S. Rahman, "Size and Concentration Analysis of Gold Nanoparticles With Ultraviolet-Visible Spectroscopy," Undergrad. J. Math. Model. One + Two **7**(1), (2016).
24. K. Saha, S. S. Agasti, C. Kim, X. Li, and V. M. Rotello, "Gold nanoparticles in chemical and biological sensing," Chem. Rev. **112**(5), 2739–2779 (2012).
25. J. Ou, Z. Zhou, Z. Chen, and H. Tan, "Optical diagnostic based on functionalized gold nanoparticles," Int. J. Mol. Sci. **20**(18), (2019).
26. P. N. Colloids, E. Tomaszewska, K. Soliwoda, K. Kadziola, B. Tkacz-szczesna, G. Celichowski, M. Cichomski, W. Szmaja, and J. Grobelny, "Detection Limits of DLS and UV-Vis Spectroscopy in Characterization of Detection Limits of DLS and UV-Vis Spectroscopy in Characterization of Polydisperse Nanoparticles Colloids," (February 2014), (2013).